A Bayesian Track-before-Detect Algorithm for IR Point Target Detection

Robert C. Warren

Weapons Systems Division
Aeronautical and Maritime Research Laboratory

DSTO-TR-1281

ABSTRACT

An algorithm has been developed for the detection of point targets in uncluttered background based on a Bayesian track before detect method. The algorithm has an application in the detection of sea skimming antiship missiles at maximum range, when the missile appears over the horizon. Because of the long range, angular motion of the target will be insignificant, and target motion cannot be used to aid detection. The effect of filtering with a number of spatial filters on detection efficiency is assessed. The algorithm was tested on an infrared image sequence of an aircraft approaching the sensor at low level over water with a diffuse cloud background, and it was found to perform significantly better than simple detection by threshold exceedance. The algorithm is intended for application on a massively parallel processor where each pixel is assigned to a processing element, and each pixel is considered to be an individual sensor.

RELEASE LIMITATION

Approved for public release

DEPARTMENT OF DEFENCE
DEFENCE SCIENCE & TECHNOLOGY ORGANISATION
DSTO

Published by

DSTO Aeronautical and Maritime Research Laboratory
506 Lorimer St
Fishermans Bend, Victoria 3207 Australia

Telephone: (03) 9626 7000
Fax: (03) 9626 7999
© Commonwealth of Australia 2002
AR-012-164
February 2002

APPROVED FOR PUBLIC RELEASE

A Bayesian Track-before-Detect Algorithm for IR Point Target Detection

Executive Summary

There exists a requirement to improve the capability of surface ships to detect the approach of anti-ship sea-skimming missiles (ASMs) in circumstances where ducting phenomena may prevent detection by radar, or when a quiet electromagnetic environment must be maintained. Infrared search and track (IRST) systems have been developed to fill this gap. Current generation systems are based on a scanning sensor with update rates of the order of 1 Hz. The scanning method limits the time spent at any one pixel to the order of microseconds, which gives a low signal level and a poor signal-noise ratio. The next generation systems will be based on staring array sensors, which will have much longer integration times and higher update rates, and so will have a considerable increase in detection and tracking capability.

This paper presents an algorithm for processing image sequences for possible use in IRST systems for detecting ASMs as they appear on the horizon. The aim is to obtain the earliest possible detection when the target is very dim and of subpixel size. Because of the long range, angular motion of the target will be insignificant, and target motion cannot be used to aid detection. This situation requires fundamentally different processing procedures from the detection of moving targets.

Since only the region near the horizon is of interest, the area to be scanned, and hence the number of pixels, is much reduced. In this case it is feasible to use a massively parallel processor, and to associate a single processing element of the processor with each pixel. In this case each pixel-processing element combination becomes an individual sensor. The algorithm will use spatial filters to reduce the magnitude of clutter and temporally decorrelate the residual clutter, and a Bayesian likelihood track before detect (TBD) process for target detection. This technique calculates the likelihood that the target exists at a pixel, and accumulates the likelihood as each frame is processed. When the likelihood exceeds a threshold a detection is declared.

The algorithm was tested on an infrared image sequence of an aircraft approaching the sensor at low level over water with a diffuse cloud background. The algorithm was found to perform significantly better than simple detection by threshold exceedance.

Authors

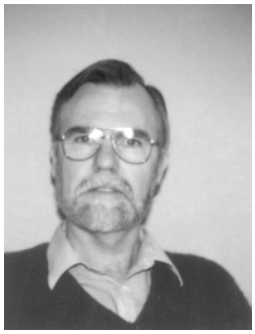

Robert C. Warren
Weapons Systems Division

Bob Warren obtained an MSc in Physics from the University of NSW in 1969. After joining what became DSTO in 1968 he worked in the fields of X-ray crystallograpghy, neutron diffraction and X-ray fluorescence spectroscopy. On moving to Salisbury in 1972 he worked on the mechanical properties of composite and nitrocellulose based propellants. After a 2 year attachment in the UK, he made discoveries in the mechanical relaxation and rheological behaviour of nitrocellulose materials. After a spell working on the prediction of rocket exhaust flowfields, he is now in the Advanced Concepts Group working on IR search and track systems.

Contents

1. Introduction

There exists a requirement to improve the capability of surface ships to detect the approach of anti-ship sea-skimming missiles (ASMs) in circumstances where ducting phenomena may prevent detection by radar, or when a quiet electromagnetic environment must be maintained. Infrared search and track (IRST) systems have been developed to fill this gap. Current generation systems are based on a scanning sensor with update rates of the order of 1 Hz. The scanning method limits the time spent at any one pixel to the order of microseconds, which gives a low signal level and a poor signal-noise ratio. The next generation systems will be based on staring array sensors, which will have much longer integration times and higher update rates, and so will have a considerable increase in detection and tracking capability.

This paper will present an algorithm for processing image sequences for possible use in IRST systems for detecting ASMs as they appear on the horizon. The emphasis is on the Bayesian track before detect (TBD) component of the algorithm. The method relies on assumptions on the nature of the sensor and the philosophy of use.

An IRST can be used to:- a) detect sea skimming missiles as they appear over the horizon, and also b) to track manoeuvring targets at closer ranges. Current systems combine these operations in one process and processor, but these cases have conflicting requirements. Details of these requirements are as follows.

a) Detection of sea skimming missiles as they appear over the horizon.
Only a small region of the total field within approx 0.2° of the horizon needs to be scanned. The angular motion of the target at maximum range is near zero, so target motion cannot be used to aid detection. The target will be very dim and scintillating, so the detector will have to be robust against random disappearances of the signal. The requirement is to detect the target at maximum range and specify its angular position. Tracking as the missile approaches could be accomplished by passing the detections to the tracking system in case b.

b) Tracking manoeuvring targets at closer ranges.
A large region of the sea and sky needs to be scanned. The targets will be relatively bright and will probably have a significant angular velocity. Detection should be relatively straightforward because of their greater brightness, and the main processing requirement is for tracking.

These considerations indicate that the two cases require fundamentally different processing procedures, and probably different processors optimised for each purpose.

A second generation IRST will possibly be based on a focal plane array (FPA) of 2000×2000 pixels. Using an anamorphic lens with a ratio of 3 to 1, a field of view 60°x20° can be mapped onto the FPA, with each pixel representing a horizontal rectangle with aspect ratio 3x1. This would give a resolution of 100pixels/° in the vertical direction and 33 pixels/° in the horizontal direction.

To obtain an estimate of the processing power required for ASM detection, assume that the mapping to the IRST FPA is 100 pixels/°, or 1 pixel subtends 0.17 mrad, that

a target has to be detectable from the horizon to 10 km, and that the maximum height of interest is 20 m. This situation corresponds to a vertical angular range of 2 mrad, or 0.115°, or 12 pixels. If 6 sensors are used to cover the whole horizon, the horizontal angular range for each sensor is 60°, or 1980 pixels. The total number of pixels for each sensor to be analysed is then 24,000.

This number of sensors makes it feasible to use a massively parallel processor, and to associate a single processing element with each pixel. In this case each pixel-processing element becomes an individual sensor. This paper will develop and evaluate an algorithm for detection of targets for the situation described above which are suitable for parallel processing. The algorithm will use spatial filters to reduce the magnitude of clutter and temporally decorrelate the residual clutter, and a Bayesian TBD process for target detection.

The detection procedure involves first spatially filtering the image sequence to accentuate point-like objects and temporally decorrelate residual clutter at each pixel. Non-linear spatial filters based on medians or Mathematical Morphology operators are candidate filters for detection of dim point targets in IR image sequences. Both median subtraction filters and filters based on erosions and dilations have been used [1-7]. These filters are related, as median filtering can be achieved by a combination of erosions. Median filtering in 1D is well understood, but the generalisation to 2D is not straight forward. Arce and McLoughlin[8] showed that the standard square window which is often used gave a greater loss of resolution of small features than the Max/Median filter, which consisted of the maximum of a series of linear filters through the point of interest. The Max/Median filters have a high computational load and will not be used here.

Three and five pixel horizontal and vertical linear elements and a 3x3 pixel square element will be evaluated in this paper. Preliminary work showed that the most effective simple morphological filters were openings and a closing filter followed by an opening filter. The same elements as used for the median filters will be used for morphological structuring elements.

Temporal filters have also been used for target detection. Most examples of temporal filtering in the literature have assumed that the target has a significant angular velocity with respect to the sensor. One such filter is described by Tzannes and Brooks[9]. However, the assumption is that the angular motion of targets at the horizon is negligible, so these types of filter are not useable.

An efficient Bayesian TBD technique has been developed by Arnold et al [10]. A detailed description of Bayesian methods for target detection and tracking has been given by Stone et al [11]. Bayesian TBD techniques have been applied to IRST systems by Branlund et al[12] and Merlo et al[13]. The application was to tracking as well as detection, as the IRST systems were scanning types with an update time of 0.5 to 1 second. At this low rate the target could move significantly between frames and so sophisticated tracking is necessary, but the time available for computation would also be longer and so the more complex methods would be practical. In the current work it is assumed that the target has very small motion and that the frame rate is high, so that tracking of the target is not difficult, but target detection is the major

problem. In these circumstances it is possible to drastically reduce the complexity of the Bayesian likelihood calculation.

2. Experimental

Spatial and temporal filtering methods will be evaluated using an image sequence of an aircraft approaching the infrared camera over water at an altitude of approximately 30 m over Gulf St Vincent off Adelaide. The effective target was the front surfaces of the twin exhaust pipes of the aircraft.

Image sequences to be analysed were obtained using an Amber Galileo midwave infrared camera. The Galileo focal plane array consists of 256x256 pixels, each pixel a square 30 μm on side. The infrared camera was fitted with a 300 mm catadioptric lens and operated at 25 frames/s. The 300 mm lens gives a pixel size of 0.1 mrad, or 0.00573°, giving 175 pixels/°. The field of view (FOV) is 1.467° in horizontal and vertical directions.

The Gabriel software (Aspect Computing, Adelaide, Australia) was used to display image sequences, and also to measure pixel intensities and means and standard deviations of image areas. Image filtering and processing were done with specially written C programs.

3. Spatial Filtering

Various median and morphological filters have been used for dim point target detection, and in this work the median subtraction filter will be referred to as the median filter. In the literature filters have often used a relatively large number of elements. In the present case only a single pixel target is of interest, and since low computational load is a requirement, filters with only a few elements will be considered. The filters chosen for study were:-

a. Morphological, Opening, 3 pixel horizontal element – Op3.
b. Morphological, Close-open, 3 pixel horizontal element – Co3h.
c. Median, 3 pixel horizontal element – Dm3h.
d. Morphological, Close-open, 3 pixel vertical element – Co3v.
e. Median, 3 pixel vertical element – Dm3v.
f. Morphological, Close-open, 5 pixel horizontal element – Co5h.
g. Median, 5 pixel horizontal element – Dm5h.
h. Morphological, Close-open, 5 pixel vertical element – Co5v.
i. Median, 5 pixel vertical element – Dm5v.
j. Morphological, Close-open, 3x3 pixel element Co9.

In the cases of 3 and 5 pixel linear elements the results of the horizontal and vertical filtering were combined. Only detections occurring in both filter outputs were counted.

4. Track before Detect Method

The sequence resulting from the spatial filtering was subjected to a track before detect process. A target detection was declared when the target likelihood exceeded a threshold.

The aim is to detect the weakest possible target signal at maximum range. A target will have very small angular motion, and will be assumed to be confined to 1 pixel. Scintillation or pixelation effects may spread the target over at most 3 pixels, but usually only one pixel is bright. Scintillation also causes the target signal to fluctuate wildly, and a detection method must be robust against missed detections. Each pixel will be considered to be an individual sensor. Only one target would be present to a sensor at any time. Detection will be made by calculating the likelihood of target presence at a pixel location by a Bayesian procedure described by Stone et al [11] and summarised in the Appendix.

The basic equation for calculating target likelihood at a particular pixel location is

$$\ln \Lambda^*(t_k, s) = r y_k - \frac{r^2}{2} + \ln \Lambda^*(t_{k-1}, s)$$

where y_k is the current iteration pixel intensity, r the parameter describing the sensitivity of detection, usually taken as a multiple of the standard deviation of the background, t_k is the time at iteration number k, and Λ is the likelihood. A full derivation and explanation of the log likelihood calculation is given in the Appendix. It is assumed that the data has been rescaled so that the background has zero mean. The method also assumes that the background and target intensity distributions are Gaussian, and this is usually true for the background. However, because of the effects of scintillation the target intensity distribution is log Gaussian [14]. This difference will be ignored here, but its effect would be to increase the sensitivity of the method.

If the calculation of likelihood is allowed to proceed unchecked as the image sequence is processed, the likelihood in background regions would drop to very low values, and when a target appeared it would take an inordinate amount of time for the likelihood to build up to detectable levels. Hence it is necessary to set a minimum allowable value for the likelihood. Similarly strong, brief false alarms could build up sufficient likelihood to be detected as a target and persist for long times, so a maximum allowable value of likelihood needs to be set. These maximum and minimum values are extra parameters which need to be specified.

It was decided to select 1 second as the time to allow likelihood to build up for detection, and this corresponded to 25 frames. The minium allowed likelihood value was set to the value that the background would achieve after 25 frames, and the maximum value was set to the value that a target value of r would achieve in 25 frames. Once a detection was declared, a variable denoting the strength of the declaration was increased by 1 for each frame in which a detection occurred to a maximum excess of 12. For each frame where the likelihood dropped below the detection level the variable was reduced by 1. This ensures that if the target disappears, the detection would lapse after 0.5 seconds, but would still make the algorithm robust against the effects of target scintillation.

The resulting procedure is as follows. The background standard deviation is determined or estimated and the value of r calculated, and it is used to calculate the

maximum and minimum values. The initial likelihood is set to 0, and the image sequence processed. A detection is declared when the likelihood exceeds 0 and is dropped when the likelihood drops below 0.

5. Results

The target aircraft carried a GPS unit, and the actual trajectory was recorded at 1 second intervals. There was significant drift in bearing during the flight. The background sky consisted of only very light distant high level cloud cover.

The resolution of the original image sequence was 175 pixels/°, which was significantly higher than the assumed IRST being simulated. The resolution was reduced by resampling with the average of 2x2 pixels of the original image. This procedure ignores the effect of the lens optical transfer function on the image, but the result was considered to be suitable for the current analysis because the point spread was expected to be less than the enlarged pixel size.

Because of the drift in bearing during the flight the target image moved over a number of pixels, which is contrary to the assumption made for a target in a real IRST. An apparently stationary target location was produced using the following procedure. The target was manually tracked during the periods when it was visible. The values of the target pixel and a small surrounding area were copied to a fixed location using knowledge of the true track. The local mean around the target location and the local mean at the fixed location were calculated, and the copied values were adjusted to allow for the difference in means. The intensity at the old target location was replaced with the average local intensity.

The last frame of the sequence showing the target is given in Figure 1. As well as the target there is a grain silo on the horizon on the other side of the body of water. The silo has a width of 1 pixel , which would be expected to pass the horizontal filters. The bright spot near the centre is a bird, and the target is barely visible about 15 mm above and to the left of the bird. The bright area in the foreground is a stone breakwater. The lower intensity of the sky in the centre is a result of drift in the calibration of the camera.

The intensity of the target pixel vs frame number is illustrated in Figure 2. The target is introduced in frame 725. The average intensity increase at the target pixel at the end of the sequence is less than 20 counts above the background of about 3630.

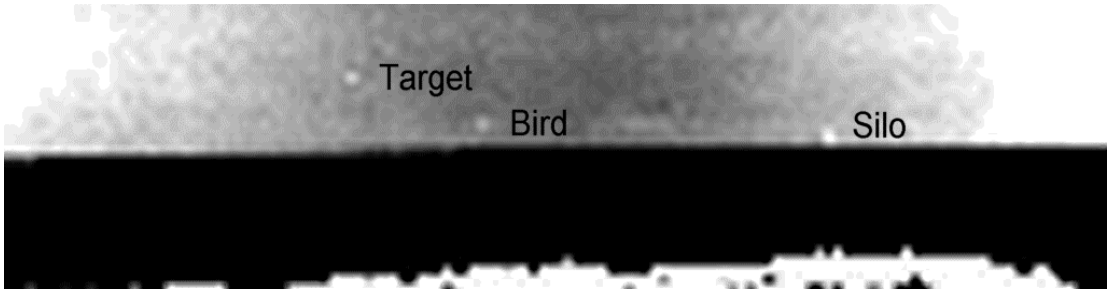

Figure 1. Last frame of image sequence.

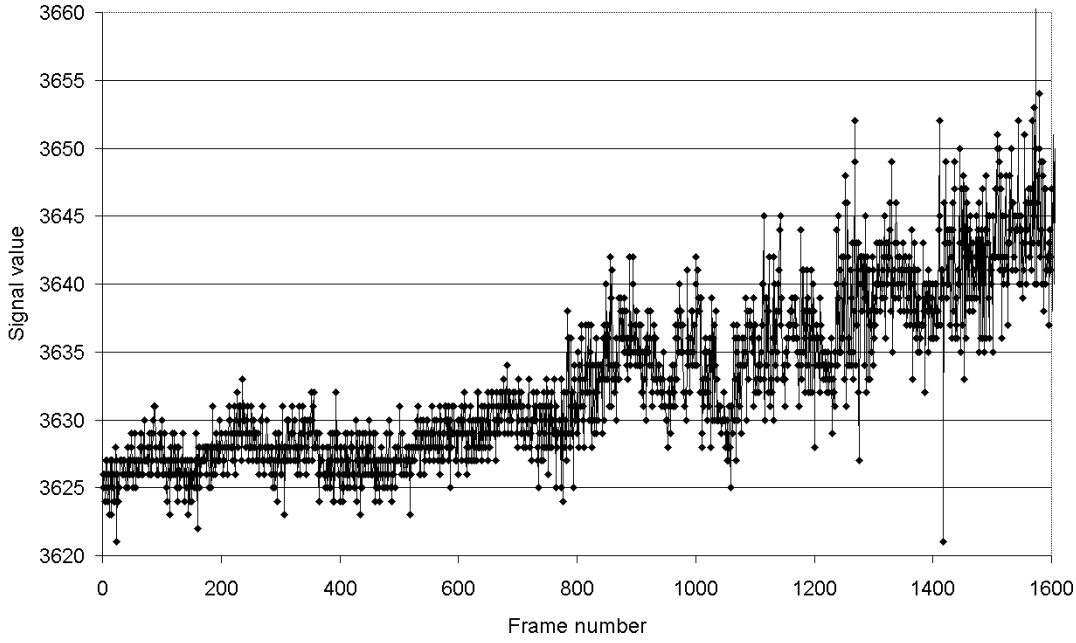

Figure 2. Target intensity vs frame number.

Table 1. Filter parameters, target detections and false alarms for the spatial filters.

Filter	Background mean	Background std. dev.	Min	Max	Targets	False alarms	Fa/frame
Op3h	0.6	1.2	-108	36	744	54457	33.51
Op3v	0.83	1.4	-156	40	697	40856	25.14
op3c					680	6516	4.01
co3h	-0.49	1.32	-55	119	733	31861	19.61
co3v	-0.28	1.6	-106	150	753	54665	33.64
co3c					730	5904	3.63
dm3h	0	1.43	-102	102	705	30684	18.88
dm3v	0.1	1.41	-106	92	734	22152	13.63
dm3c					679	4398	2.71
co5h	-0.87	1.55	-53	188	728	19560	12.04
co5v	-0.59	1.86	-118	228	737	35643	21.93
co5c					723	6323	3.89
dm5h	0	1.55	-120	120	736	46603	28.68
dm5v	0.24	1.76	-176	134	749	47054	28.96
dmc					731	7341	4.52
co9	-0.74	1.82	-98	233	741	78987	48.61

The area of interest for detection of sea skimming missiles is from 2 pixels below the horizon to 8 pixels above the horizon. This is the area that was used to determine the detection vs false alarm rate efficiency of the various spatial filters. Since the target was expected to be seen against a sky background, the background statistics were obtained from the sky region. A similar process could be carried out for the sea if the target was below the horizon, although this would not occur in most engagement geometries.

The filter parameters and results are summarised in Table 1. The value of the parameter r was chosen to be twice the standard deviation of the output of the appropriate filter in the background area. The "c" designated the combined output of the 2 linear filters.

More details of target detection are given in Table 2. There is not a significant difference in the first detection ability of most of the filters, and their ability to maintain detection is reflected in the number of detections given in Table 1.

Table 2. Frame numbers for detection and loss of targets.

Filter	Detect	Lose	Detect	Lose	Detect	Lose	Detect
op3c	870	952	993	1056	1082	1232	1244
co3c	882	966	980	-	-	-	-
dm3c	888	964	988	1054	1087	1235	1242
co5c	884	966	987	-	-	-	-
dm5c	876	966	978	1064	1072	-	-
co9	882	969	974	-	-	--	-

To show the working of the method, the 3 pixel median case will be discussed in detail. A plot of the filtered intensity of the target pixel is given in Figure 3. From the figure, it can be seen that the mean output for the background was approximately zero. The target appears at about frame 770, and briefly disappears near frames 1050, 1230 and 1400 due to atmospheric refraction effects with a longer timescale than scintillation. This sequence provides a difficult test for the TBD process, as it must track the intensity variations in a balanced way. It must not drop a target which disappears only a few frames, and it must not maintain a detection for unduly long after it has really disappeared. It is worth noting that several birds flew across the field of view, but these were not detected as false alarms because they were at any pixel for less than the integration time.

The output images of the detections from the horizontal and vertical 3 element linear median filters, and the combined output of both, are given in Figure 4. Of the 3 detections in the sky region in Figure 4, the leftmost is the target, the centre is a defective pixel in the camera, and the rightmost is the 1 pixel wide silo which is a constant in all frames.

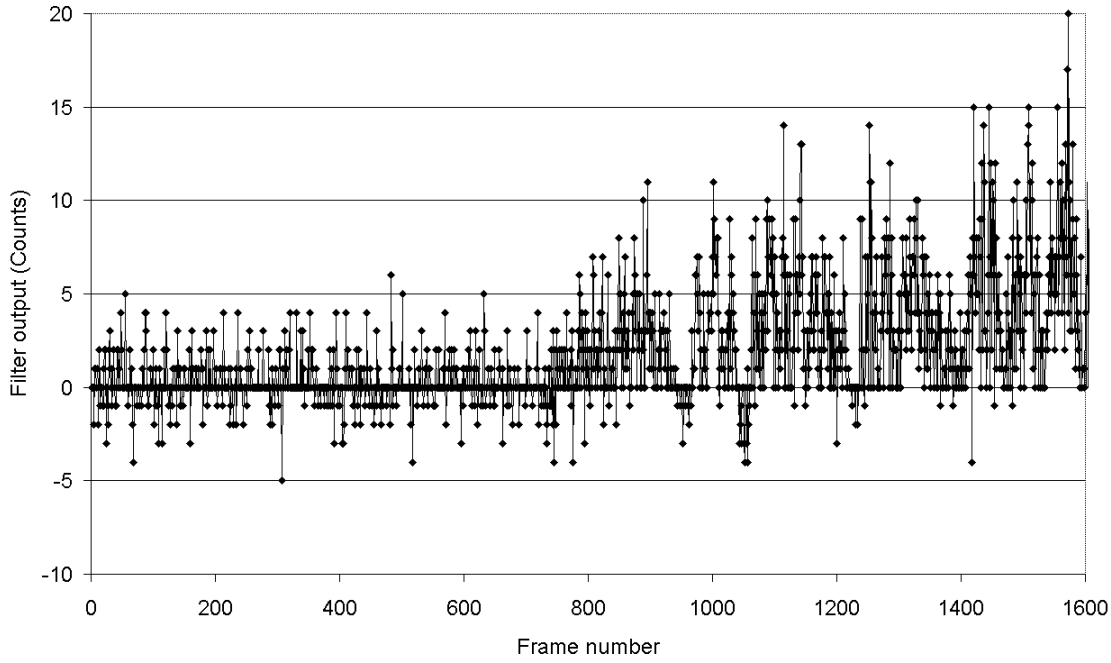

Figure 3. Plot of intensity of target pixel after 3 pixel horizontal median subtraction filter.

Table 3. Target detections and false alarms calculated from threshold exceedences.

	Threshold = 1		Threshold = 2		Threshold = 3		Threshold = 4	
Filter	Targets	False alarms	Targets	False alarms	Targets	False alarms	Targets	False alarms
op3c	-	-	872	61732	773	20033	630	7730
co3c	699	18468	610	7513	476	4522	-	-
dm3c	795	81766	662	26051	503	7877	396	2479
co5c	656	10433	506	5746	381	4090	-	-
dm5c	902	129124	787	41366	655	13633	518	6058

To show the improvement in performance obtained with the TBD method, a standard threshold exceedance calculation was made. The outputs from the various filters were thresholded at values of 1 to 4 counts, and the results from the horizontal and vertical filters were combined to give detections. The results are given in Table 3 and Figure 5. The values near 900 are likely to be affected by false alarms at the target pixel location, as visual inspection showed that there were frames where detections could not be made. If the threshold detections near below about 750 are genuine, they are obtained with a much higher number of false alarms than the TBD detections, and hence the TBD method shows clear superiority

Because the mean output from the background for each filter is not an integer, it is not possible to use the same relative value of threshold for each filter. The threshold

values in Table 3 are the absolute values. It can be seen that in comparison with Table 1 the performance of thresholding is significantly poorer than the TBD method. The false alarm rate is much higher for any level of target detection. The performance of the thresholding method using the combination of the 3 element linear median filter is illustrated in Figure 6. The average number of false alarms per frame is about 5. The rate of detection is very intermittent until about frame 1100, and is not consistent until about frame 1300.

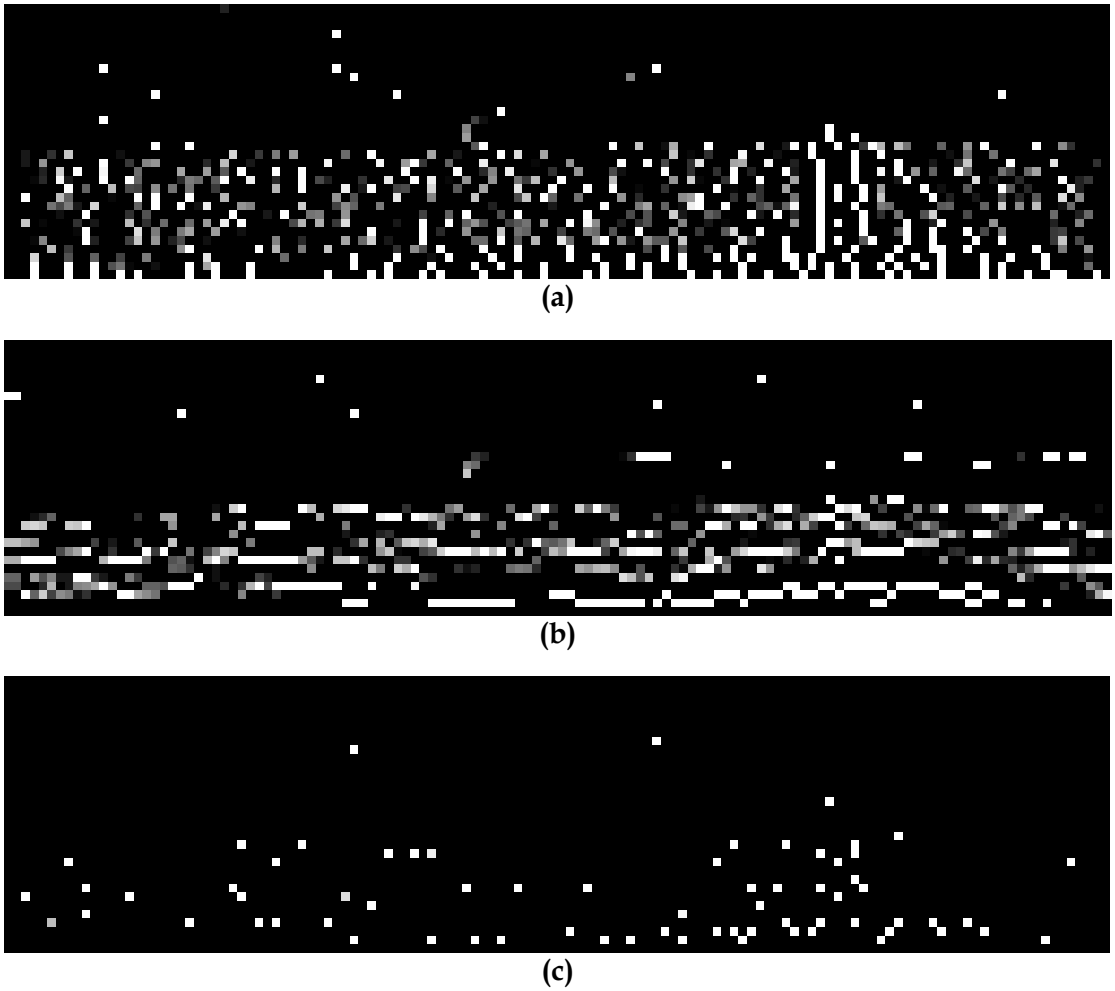

Figure 4. Outputs from the 3 element median filters for frame 1625. (a) Horizontal, (b) Vertical, and (c) Both horizontal and vertical.

6. Discussion

It can be seen from Table 1 that the best detection efficiency for a reasonable number of false alarms is given by the linear 3 element close-open filter. The 3 element median filter gave a smaller number of detections, but also a significantly smaller number of false alarms, and with tweaking of the parameters it may give a response comparable to the close-open filter. The median filter also has other advantages. The mean value of the filtered background is approximately zero, and the distribution of filtered background intensity values is near to Gaussian. This adds legitimacy to the use of the likelihood processing. All the other morphological filters gave non-zero values for the mean filtered background.

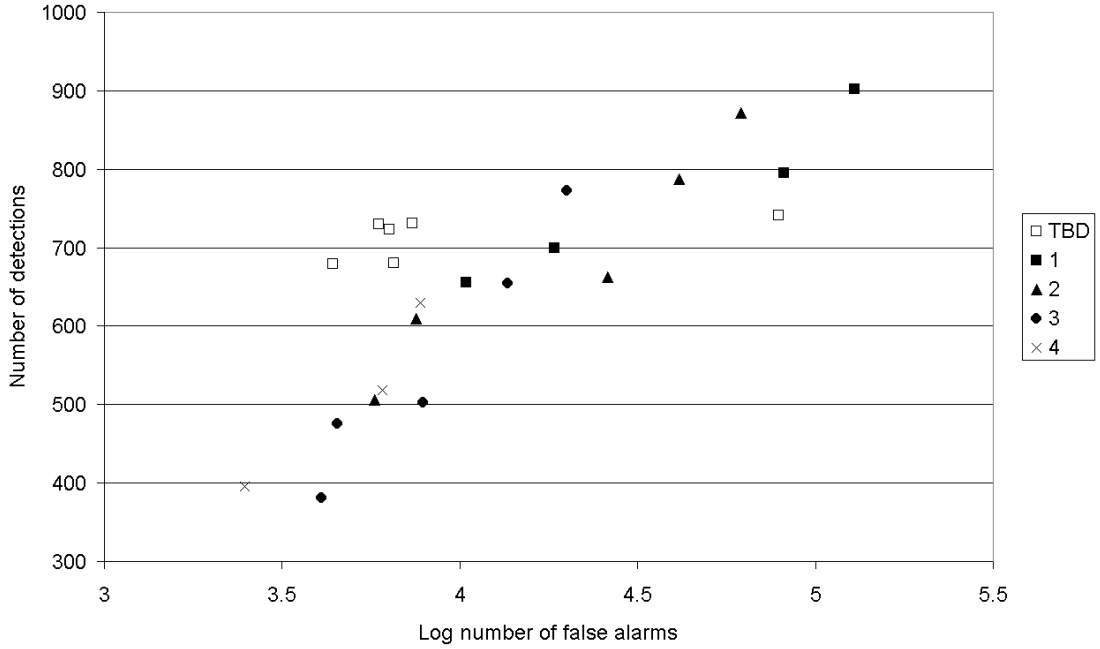

Figure 5. Number of detections vs false alarms for the TBD and threshold methods. Threshold levels given in the legend.

The detection range was not very sensitive to filter type, so the type of filter used can be chosen for computational efficiency. Because of the refraction effects in the atmosphere, it is not certain if this was the maximum possible range under the circumstances. Intensity of the target would have been relatively high as the exhaust pipes would be hot. A stealthy missile would have a lower intensity and so its detection range would be more sensitive to processing parameters. Measurements of constant intensity sources at a range of distances and under a range of environmental conditions are needed to obtain definitive maximum detection ranges.

From Figure 4 it can be seen that combining the outputs from the horizontal and vertical filters considerably reduced the number of detections in both the sky and sea regions. Similar behaviour is seen with the other filters.

The efficiency of the TBD process was considerably better than a simple thresholding process. Extra processing would have to be done on the thresholded outputs to give acceptable response. The TBD method is very computationally efficient, and would probably compare well with other methods to improve the threshold result. Also from Figure 4 it can be seen that the little cloud clutter that was present has been suppressed from the sky region. The drift in calibration of the camera also did not affect the output of the filters. Cloud clutter is relatively benign in this case and simple morphological filters were able to suppress it. It is expected that most cloud clutter on the horizon would be at very long range and would appear to be diffuse, so simple filters should suffice in most cases. However, there may be problems in directions near a low sun, but this situation would be a problem for most filters.

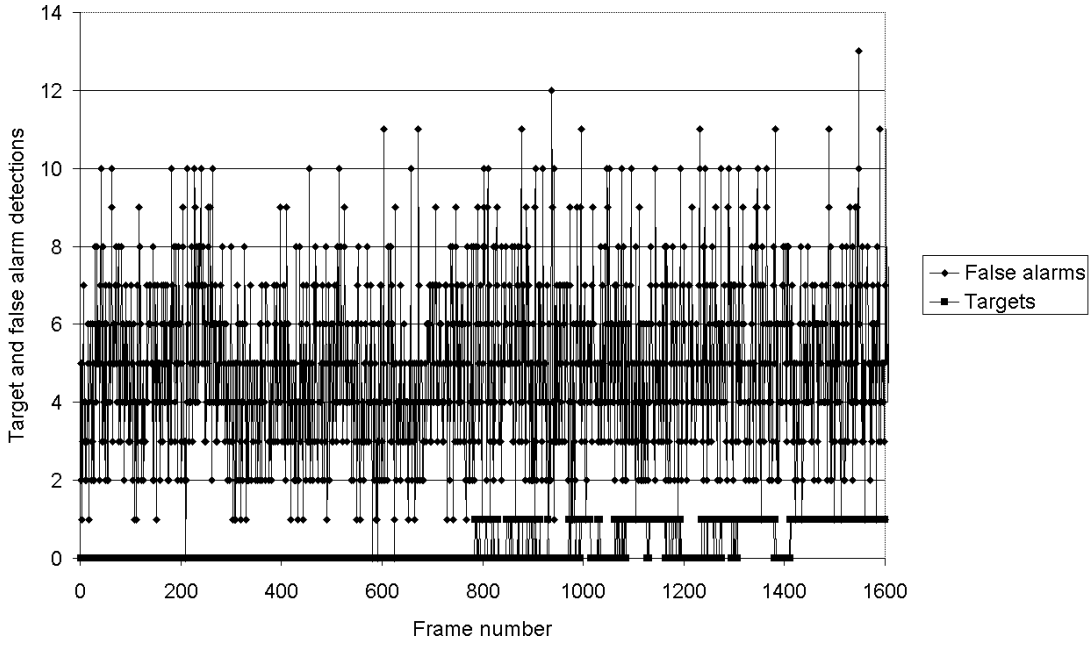

Figure 6. Target detections and false alarms from thresholded output of 3 element median filters, threshold = 3.

In the sea region there is a greater number of false alarms, but these are often short lived. The detection algorithm was optimised on the standard deviation of the sky region, and so was not optimal for the sea region. If the standard deviation of the sea intensity fluctuations was used in the algorithm the false alarms in the sea region would be much reduced, but the sensitivity to targets would also be reduced. False alarms in the sea may be better handled by using longer time constants in the TBD algorithm.

Early detection of ASMs requires the processing of very low signals, and it would be desirable to be able to make a detection when the mean of the target signal above the background is less than 1 excess count. The highly quantised nature of the signal requires a different processing philosophy, and different considerations of accuracy. Floating point capability is not necessarily an advantage.

The aim of this work is to implement the spatial filtering and TBD algorithm on a massively parallel processor. The processor under consideration is the Aspex Associative String Processor (Aspex Technology Limited, Brunel Science Park, Uxbridge, UK) . The Aspex processor consists of 1 bit adders as processing elements and 70 bits of memory per processor. The spatial filtering should be able to be implemented efficiently on the processor as the filtering involves shifts and comparisons. Some approximations would have to be made with the TBD algorithm to allow for calculation in integer arithmetic. However, the relative loss of accuracy should not be too great as the raw data consists of integer counts of low value, often less than 5 counts.

In an operational system extra intelligence would be required to facilitate the correct assignment of detections to real targets or false targets. The temporal behaviour of possible targets could be compared to expected behaviour of target intensity.

Detections with diminishing intensity would not be targets. Constant intensity pixels would be marked as defective pixels or fixed environmental clutter, and eliminated from consideration. These operations could be carried out in the serial track processor.

Trials are planned to obtain image sequences of constant intensity source at long range over water to analyse the statistics of background and targets at a range of intensities. This would allow optimisation of parameters and comparison of the effectiveness of the various spatial filters.

7. Conclusions

A simple Bayesian track-before-detect algorithm has been developed for IRST applications which shows promise for detecting ASMs at ranges near the horizon. The computational load of the basic algorithm is low, and the algorithm is suitable for implementation on a massively parallel processor. The performance is superior to simply thresholding the output of spatial filters.

Morphological filters based on short linear elements were found to effectively suppress light cloud clutter and enhance dim point target detectability.

Further work is required using constant standard sources at a number of ranges and environmental conditions to optimise the parameters in the algorithms and determine the effectiveness of the methods for IRST applications.

8. Acknowledgements

The author is pleased to acknowledge the cooperation of ARDU in the provision of aircraft and aircrew, and the aircrew SQNLDR C. Daniel and SQNLDR S. Maneschi. Stephane Collignon is thanked for his assistance with the software integration and Greg Teague for assistance with the planning and execution of the trials.

9. References

1 Tom, V. T., Peli, T., Leung, M. and Bondaryk, J. E. (1993) Morphology-based algorithm for point target detection infrared backgrounds, *Signal and Data Processing of Small Targets* SPIE 1954, Drummond, O. E. (ed) SPIE - International Society for Optical Engineering.

2 Barnett, J. T. (1989) Statistical analysis of median subtraction filtering with application to point target detection in infrared backgrounds, *Infrared Systems and Components III* SPIE 1050, Caswell, R. L. (ed) SPIE - International Society for Optical Engineering.

3 Sang, N., Zhang, T. and Wang, G. (1996) Gray scale morphology for small object detection, *Signal and Data Processing of Small Targets* SPIE 2759, Drummond, O. E. (ed) SPIE - International Society for Optical Engineering.

4 Sang, N., Zhang, T. and Shi, W. (1998) Characteristics of contrast and application for small target detection, *Signal and Data Processing of Small Targets* SPIE 3373, Drummond, O. E. (ed) SPIE - International Society for Optical Engineering.

5 Li, J., Shen, Z. and Biao, L. (1997) Detection of small moving objects in image sequences, *Automatic Target Recognition VII* SPIE 3069, Sadjadi, F. A. (ed) SPIE - International Society for Optical Engineering.

6 Barnett, J. T., Billard, B. D. and Lee, C. (1993) Nonlinear morphological processors for point-target detection versus an adaptive linear spatial filter: a performance comparison, *Signal and Data Processing of Small Targets* SPIE 1954, Drummond, O. E. (ed) SPIE - International Society for Optical Engineering.

7 Deshpande, S. D., M.H.Er, Ronda, V. and Chan, P. (1999) Max-mean and max-median filters for detection of small-targets, *Signal and Data Processing of Small Targets* SPIE 3809, Drummond, O. E. (ed) SPIE - International Society for Optical Engineering.

8 Arce, G. R. and McLoughlin, M. P. (1987) Theoretical nalysis of the max/median filter, *IEEE Transactions on Acoustics, Speech and Signal Processing* **35**(1) 60-69

9 Tzannes, A. P. and Brooks, D. H. (1999) Point target detection in IR image sequences based on target and clutter temporal profile modeling, *Infrared Technology and Applications XXV* SPIE 3698, Andresen, B. F. and Strojnik, M. (eds) SPIE - International Society for Optical Engineering.

10 Arnold, J., Shaw, S. and Pasternack, H. (1993) Efficient target tracking using dynamic programming, *IEEE Transactions on Aerospace and Electronic Systems* **29**(1) 44-56

11 Stone, L. D., Barlow, C. C. and Corwin, T., L, (1999) *Bayesian Multiple Target Tracking* Boston, Mass.,Artech House.

12 Branlund, E., Davis, P. and Lindgren, U. (1996) Infrared detection of low-contrast sea-skimming cruise missiles, *Targets and Backgrounds: Characterization and Representation II* SPIE 2742, Watkins, W. R. and Clement, D. (eds) SPIE - International Society for Optical Engineering.

13 Merlo, S. P., Lindgren, R. G. and Davis, P. J. (1997) Application of Bayesian field track-before-detect and peak likelihood track-after-detect trackers to shipboard infrared search and track, *Signal and Data Processing of Small Targets* SPIE 3163, Drummond, O. E. (ed) SPIE - International Society for Optical Engineering.

14 Hufnagel, R. E. (1985) Propagation through atmospheric turbulence. In: Wolfe, W. L. and Zissis, G. J. (eds) *The Infrared Handbook.* Office of Naval Research, Washington, D.C., pp. Chap. 6.

Appendix A: Derivation of Bayesian Track before Detect Method

A.1. Background

This derivation of the Bayesian likelihood calculation is based on reference 11.

Let S be the state space of the target, and X(t) be the target state at time t. Prior information about the target is represented by the stochastic process { X(t); t ≤ 0}.

Assume the presence of observations obtained at times $0 \le t_1 \le .. \le t_k$. Let Y_k be a random variable corresponding to the set of observations obtained at time t_k . Let y_k denote a value of the random variable Y_k. Assume that the likelihood function can be calculated as

$$L_k(y_k \mid s) = \Pr\{Y_k = y_k \mid X(t_k) = s\}$$

$$\text{Let } \mathrm{Y}(t) = (Y_1, ..., Y_K) \quad \text{and} \quad \mathrm{y} = (y_1, ..., y_K)$$

$$\text{Define } L(\mathrm{y} \mid s_1, ..., s_K) = \Pr\{\mathrm{Y}(t) = \mathrm{y} \mid X(t_1) = s_1, ..., X(t_K) = s_K\}$$

which is the probability that the observations $\mathrm{Y}(t) = \mathrm{y}$ are obtained given that the target has passed through states $s_1,\ldots,s_K$

The prior probability that the process { X(t); t ≤ 0} passes through states $s_1,\ldots,s_K$ at times $t_1,\ldots,t_K$ is defined as

$$q(s_1, ..., s_K) = \Pr\{X(t_1) = s_1, ..., X(t_K) = s_K\}$$

The posterior probability, given the observations $\mathrm{Y}(t) = \mathrm{y}$, is

$$p(t_K, s_K) = \Pr\{X(t_K) = s_K \mid \mathrm{Y}(t_K) = \mathrm{y}\}$$

Using Bayes' Theorem

$$p(t_K, s_K) = \frac{\Pr\{\mathrm{Y}(t_K) = \mathrm{y} \_ and \_ X(t_K) = s_K\}}{\Pr\{\mathrm{Y}(t_K) = \mathrm{y}\}}$$

$$= \frac{\int L(\mathrm{y} \mid s_1, ..., s_K) q(s_1, ..., s_K) ds_1 .....ds_{K-1}}{\int L(\mathrm{y} \mid s_1, ..., s_K) q(s_1, ..., s_K) ds_1 .....ds_K}$$

Two assumptions about L and q allow a recursive evaluation of $p(t_K, s_K)$:- the stochastic process { X(t); t ≤ 0} must be Markovian, and the observations at different

times must be independent of each other given $(X(t_1) = s_1, ..., X(t_K) = s_K)$. The likelihood function can then be written

$$L(\mathrm{y} \mid s_1, ..., s_K) = \prod_{k=1}^{K} L_k(y_k \mid s_k)$$

This means that the observations at a particular time depend only on the state at that time.

Define a transition function

$$q_k(s_k \mid s_{k-1}) = \Pr\{X(t_k) = s_k \mid X(t_{k-1}) = s_{k-1}\}$$

for $k \geq 1$, and q_0 is the probability density function for X(0).

Since the stochastic process $\{X(t); t \leq 0\}$ is Markovian,

$$q(s_1, ..., s_K) = \int_S \prod_{k=1}^{K} q_k(s_k \mid s_{k-1}) q_0(s_0) ds_0 \ .$$

Substituting,

$$p(t_K, s_K) = \frac{1}{C} L_K(y_K \mid s_K) \int_S q_K(s_K \mid s_{K-1}) p(t_{K-1}, s_{K-1}) ds_{K-1} \ .$$

The recursion relations become

$$p(t_0, s) = q_0(s) \text{ for } s \in S$$

for $k \geq 1$ and $s \in S$

Motion update

$$p^-(t_k, s_k) = \int_{S+} q(s_k \mid s_{k-1}) p(t_{k-1}, s_{k-1}) ds_{k-1}$$

Information update

$$p(t_k, s) = \frac{1}{C} L_k(y_k \mid s) p^-(t_k, s)$$

To allow for the target not existing in any of the states of S, augment the target space to S+ with the null state ϕ. Assuming at most one target in S,

$$p(\phi) + \int_{s \in S} p(s) ds = 1$$

The formalism then becomes

$$p^-(t_k, s_k) = \int_{S+} q(s_k \mid s_{k-1}) p(t_{k-1}, s_{k-1}) ds_{k-1} \text{ for } s \in S+$$

$$p(t_k, s) = \frac{p^-(t_k, s) L_k(y_k \mid s)}{C(k)} \text{ for } s \in S$$

$$p(t_k, \phi) = \frac{p^-(t_k, \phi) L_k(y_k \mid \phi)}{C(k)}$$

$$C(k) = p^-(t_k, \phi) L_k(y_k \mid \phi) + \int_{s \in S} p^-(t_k, s) L_k(y_k \mid s) ds$$

Define the target likelihood ratio, $\Lambda(s)$.

$$\Lambda(s) = \frac{p(s)}{p(\phi)} \quad \text{for } s \in S$$

$$\Lambda(t, s) = \frac{p(t, s)}{p(t, \phi)}$$

$$\Lambda^-(t, s) = \frac{p^-(t, s)}{p^-(t, \phi)}$$

And the measurement likelihood ratio

$$\mathrm{L}_k(y \mid s) = \frac{L_k(y \mid s)}{L_k(y \mid \phi)} \quad \text{for } y \in H_k,\ s \in S$$

If it can be assumed or organised that

$$p^-(t_k, \phi) = q_k(\phi \mid \phi) p(t_{k-1}, \phi) + \int_S q_k(\phi \mid s) p(t_{k-1}, s) ds = p(t_{k-1}, \phi)$$

$$\text{then} \quad \Lambda^-(t_k, s_k) = q_k(s_k \mid \phi) + \int_S q_k(s_k, s) \Lambda(t_{k-1}, s) ds \quad \text{for } s \in S.$$

A likelihood recursion ratio recursion can then be written

$$\Lambda(t_0, s) = \frac{p(t_0, s)}{p(t_0, \phi)} \qquad \text{for } s \in S$$

Motion update

$$\Lambda^-(t_k, s_k) = q_k(s_k \mid \phi) + \int_S q_k(s_k, s_{k-1}) \Lambda(t_{k-1}, s) ds_{k-1}$$

Information update

$$\Lambda(t_k, s) = \mathrm{L}_k(y_k \mid s) \Lambda^-(t_k, s)$$

Taking natural logarithms

$$\ln \Lambda(t_k, s) = \ln \Lambda^-(t_k, s) + \ln \mathrm{L}_k(y_k \mid s) \qquad \text{for } s \in S$$

A.2. Application of the Bayesian formalism to detection of sea skimming missiles.

The aim is to detect the weakest possible target signal at maximum range. A target will have very small angular motion, and will be assumed to be confined to 1 pixel. Scintillation or pixelation effects may spread the target over at most 3 pixels, but this effect will be ignored here. Each pixel will be considered to be an individual sensor. Only one target would be present at any time, so for each pixel there are only 2 states, target absent or target present, X(t) = ϕ or s.

Initially it will be assumed that the chance of a state changing due to "motion" factors will be very small, and the values of $q(s_k, s_{k-1})$ will be given by

$$q(s,s) = 1-\delta$$
$$q(s,\varphi) = \delta$$
$$q(\varphi,s) = \delta$$
$$q(\varphi,\varphi) = 1-\delta$$

where δ is a small fraction.

The integrals in the function definitions now become summations over 2 terms.

$$p^-(t_k, s_k) = q(s_k, s)p(t_{k-1}, s) + q(s_k, \varphi)p(t_{k-1}, \varphi)$$

$$p^-(t_k, s) = q(s,s)p(t_{k-1}, s) + q(s,\varphi)p(t_{k-1}, \varphi) = (1-\delta)p(t_{k-1}, s) + \delta p(t_{k-1}, \varphi)$$

$$p^-(t_k, \varphi) = q(\varphi,s)p(t_{k-1}, s) + q(\varphi,\varphi)p(t_{k-1}, \varphi) = \delta p(t_{k-1}, s) + (1-\delta)p(t_{k-1}, \varphi)$$

The posterior probabilities are then

$$p(t_k, s) = \frac{L_k(y_k \mid s)p^-(t_k, s)}{C(k)} = \frac{L_k(y_k \mid s)[(1-\delta)p(t_{k-1}, s) + \delta p(t_{k-1}, \varphi)]}{C(k)}$$
$$p(t_k, \varphi) = \frac{L_k(y_k \mid \varphi)p^-(t_k, \phi)}{C(k)} = \frac{L_k(y_k \mid \varphi)[\delta p(t_{k-1}, s)] + (1-\delta)p(t_{k-1}, \varphi)}{C(k)}$$

Recalling

$$\Lambda(t,s) = \frac{p(t,s)}{p(t,\varphi)} \quad \text{and} \quad \Lambda^-(t,s) = \frac{p^-(t,s)}{p^-(t,\varphi)}$$

$$\Lambda(t,s) = \frac{L_k(y_k \mid s)[(1-\delta)p(t_{k-1}, s) + \delta p(t_{k-1}, \varphi)]}{L_k(y_k \mid \varphi)[\delta p(t_{k-1}, s) + (1-\delta)p(t_{k-1}, \varphi)]}$$

Dividing by $p(t_{k-1}, \varphi)$ gives

$$\Lambda(t,s) = \frac{L_k(y_k \mid s)\left[(1-\delta)\Lambda^-(t_{k-1},s)+\delta\right]}{L_k(y_k \mid \varphi)\left[\delta\Lambda^-(t_{k-1},s)+(1-\delta)\right]}$$

Since δ is assumed to be very small, approximate $\Lambda(t,s)$ by setting δ = 0.

$$\Lambda(t,s) \approx \frac{L_k(y_k \mid s)\Lambda^-(t_{k-1},s)}{L_k(y_k \mid \varphi)} \quad \text{and}$$

$$\ln\Lambda(t,s) \approx \ln L_k(y_k \mid s) - \ln L_k(y_k \mid \varphi) + \Lambda^-(t_{k-1},s)$$

Assume the background noise has a zero mean Gaussian distribution with standard deviation σ, and the target signal has a Gaussian distribution with mean r and standard deviation σ.

$$\ln L_k(y_k \mid \varphi) = \ln\left[\frac{1}{K}\exp\left(\frac{-y_k^2}{2\sigma^2}\right)\right] = \frac{-y_k^2}{2\sigma^2} - K \quad \text{and}$$

$$\ln L_k(y_k \mid s) = \ln\left[\frac{1}{K}\exp\left(\frac{-(y_k-r)^2}{2\sigma^2}\right)\right] = \frac{-(y_k-r)^2}{2\sigma^2} - K$$

therefore

$$\ln\Lambda(t_k,s) = \frac{ry_k}{\sigma^2} - \frac{r^2}{2\sigma^2} + \ln\Lambda(t_{k-1},s)$$

A target could be declared when the log likelihood ratio exceeds a given threshold, and declared lost when the ratio drops below a threshold.

Rescaling the log ratio

$$\ln\Lambda^*(t_k,s) = \sigma^2 \ln\Lambda(t_k,s)$$

$$\ln\Lambda^*(t_k,s) = ry_k - \frac{r^2}{2} + \ln\Lambda^*(t_{k-1},s)$$

If the threshold level is rescaled, detections can be declared in the usual manner.

DEFENCE SCIENCE AND TECHNOLOGY ORGANISATION
DOCUMENT CONTROL DATA

1. PRIVACY MARKING/CAVEAT (OF DOCUMENT)

2. TITLE

A Bayesian Track-before-Detect Algorithm for IR Point Target Detection

3. SECURITY CLASSIFICATION (FOR UNCLASSIFIED REPORTS THAT ARE LIMITED RELEASE USE (L) NEXT TO DOCUMENT CLASSIFICATION)

Document (U)
Title (U)
Abstract (U)

4. AUTHOR(S)

Robert C. Warren

5. CORPORATE AUTHOR

Aeronautical and Maritime Research Laboratory
506 Lorimer St
Fishermans Bend Victoria 3207 Australia

6a. DSTO NUMBER	6b. AR NUMBER	6c. TYPE OF REPORT	7. DOCUMENT DATE
DSTO-TR-1281	AR-012-164	Technical Report	February 2002

8. FILE NUMBER	9. TASK NUMBER	10. TASK SPONSOR	11. NO. OF PAGES	12. NO. OF REFERENCES
J95055/19/219	NAV 00/109	DGMD	20	14

13. URL on the World Wide

http://www.dsto.defence.gov.au/corporate/reports/DSTO-TR-1281.pdf

14. RELEASE AUTHORITY

Chief, Weapons Systems Division

15. SECONDARY RELEASE STATEMENT OF THIS DOCUMENT

Approved for public release

OVERSEAS ENQUIRIES OUTSIDE STATED LIMITATIONS SHOULD BE REFERRED THROUGH DOCUMENT EXCHANGE, PO BOX 1500, SALISBURY, SA 5108

16. DELIBERATE ANNOUNCEMENT

No Limitations

17. CASUAL ANNOUNCEMENT Yes

18. DEFTEST DESCRIPTORS

Infrared detectors, Infrared tracking, Target acquisition, Antiship missiles, Sea skimming missiles, Bayes Theorem, Algorithms

19. ABSTRACT

An algorithm has been developed for the detection of point targets in uncluttered background based on a Bayesian track before detect method. The algorithm has an application in the detection of sea skimming antiship missiles at maximum range, when the missile appears over the horizon. Because of the long range, angular motion of the target will be insignificant, and target motion cannot be used to aid detection. The effect of filtering with a number of spatial filters on detection efficiency is assessed. The algorithm was tested on an infrared image sequence of an aircraft approaching the sensor at low level over water with a diffuse cloud background, and it was found to perform significantly better than simple detection by threshold exceedance. The algorithm is intended for application on a massively parallel processor where each pixel is assigned to a processing element, and each pixel is considered to be an individual sensor.